Determination of soil parameters in hydraulic flow model for porous media

Jozef Kačur, Patrik Mihala, and Michal Tóth

***Abstract* —** Determination of soil parameters (in fundamental flow characteristics) is investigated under new scenario in laboratory experiments with 3D samples. Infiltration into a sample is realized under the gravitation and centrifugal driven forces. Mathematical model for the flow in an unsaturated-saturated porous media is expressed in terms of Richard's equation based on the van Genuchten/Mualem experimental capillary-pressure model. Soil parameters characterize the specific porous material and are used as input data in this capillary-pressure flow model. Objective of this paper is threefold. The first is to present a direct and inverse efficient solver for governing mathematical model. The second is to apply the inverse solver for parameter estimation using only noninvasive inflow/outflow transient measurements. The third is to avoid resp. significantly reduce the creation of preferred streamlines which shadow reliability in solution of inverse problem. In our set-up, a sample of cylindrical shape is submerged in water chamber and the water infiltrates into it. The top of the cylinder is isolated and from its bottom water flows out to the collection chamber. Both chambers except of the sample bottom (resp. its part) are mutually isolated. The flux from lateral boundary into the sample is orthogonal to the driving forces in gravitation and centrifugation mode. This unlike in 1D samples (in the form of thin tubes) the creation of preferred stream lines arising due to small inhomogenities is decreased significantly. Additionally, the isolation of the 1D tube, especially in centrifugation mode, is difficult task. In centrifugation mode we can obtain additional informations from transient monitoring of centrifugal force which is also noninvasive. In our 3D experiments we are able to create more infiltration scenarios by suitable change of boundary conditions and rotational speed. Two different numerical methods have been developed. One is based on finite volume space discretization and flexible time stepping. The obtained nonlinear algebraic system is solved by an quasinewton linearization method. The second one is based only on space discretization and the original problem is reduced to the solution of stiff, nonlinear system of ordinary differential equations which is rather large. The first method is quicker and therefore is used in solving inverse problems. In our numerical experiments we demonstrate applicability of our method. The accuracy and effectiveness of our numerical method and experimental scenario are able to compensate the absence of measurements of pressure/saturation distribution inside the sample.

***Keywords* —** water transport, unsaturated porous media, soil parameters, scaling of mathematical model, gravitation and centrifugal forces

I. Introduction

HEAT and water transport models for unsaturated-saturated porous media consist of a couplet system of elliptic-parabolic partial differential equations expressing conservation of mass and energy. The fundamental part is represented by the water flow which enables the energy-mass transport. In order to predict the flow in soils, the soil hydraulic properties expressed in terms of soil parameters have to be known. These parameters are input data in the governing mathematical model for the flow. Very complex mathematical models for the flow and mass transport in unsaturated-saturated porous media are well known and analyzed in many monographs, e.g. in [1], with a vast list of quotations.

The water flow model is expressed in terms of saturation and pressure head in Richard's equation (see (1) below), which is a nonlinear and degenerate elliptic-parabolic equation with free boundaries between fully saturated and partially saturated zones and between dry and partially saturated zones. The soil retention and hydraulic permeability functions linking the saturation and pressure head are expressed by means of soil parameters using the van Genuchten-Mualem ansatz.

Determination of soil parameters (via solution of inverse problem) requires very precise solution of direct problem (when all model parameters are known) and additional measurements of inflow/outflow of water. In the case of centrifugation, the measurements of the inflow/outflow can be extended by the measurement of the centrifugal force in the prescribed time moments.

In Fig. 1 we sketch the experimental scenario in gravitation mode. In the mode of centrifugation we turn the model from vertical to horizontal position so that all components are positioned along the centrifuge arm. In that case we neglect the gravitational force since the centrifugal force is significantly larger.

The authors confirm support by the Slovak Research and Development Agency APVV-15-0681 and VEGA 1/0565/16.

J. Kačur is from SvF STU Bratislava, Department of Physics, Radlinského 11, 810 05, Slovakia, e-mail:Jozef.Kacur@fmph.uniba.sk

P. Mihala is from Comenius University Bratislava, Department of Mathematics, Mlynská dolina, 842 48, Slovakia, e-mail: pmihala@gmail.com

M. Tóth is from Comenius University Bratislava, Department of Mathematics, Mlynská dolina, 842 48, Slovakia, e-mail:m.toth82@gmail.com

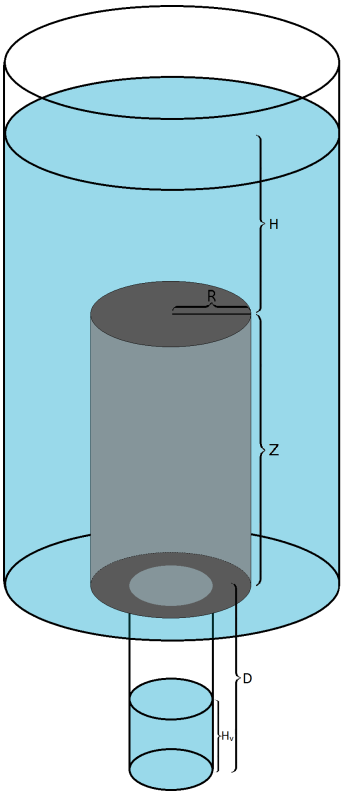

Fig. 1 Sample

In our set-up, the sample is of cylindrical shape and is submerged in the injection chamber. The water infiltrates into the sample across the lateral boundary. The top of the cylinder is isolated and water flows out to the collection chamber from its bottom. Both chambers are mutually isolated except of the sample bottom (resp. its part). Thus, the area of the inflow into the sample is much larger then in the 1D case where water inflows only at the sample top. Moreover, the isolation of the tube mantel in the 1D is technically difficult, especially in the case of centrifugation. In our 3D case the direction of the inflow flux is perpendicular to the direction of the driving force. This significantly reduces the creation of preferred stream lines.

In centrifugation mode, data collection can be accelerated. Moreover, additional measurement can be achieved by monitoring centrifugal force. The dynamics in the measured characteristics can be amplified by increase of the centrifugation speed. The measurements of the centrifugal force can be relatively simply realized keeping in ballance the centrifugal force on the opaque centrifuge arm.

Determination of soil parameters have been investigated more then two decades in both gravitation and centrifugation mode. First experiments have been explored in saturated samples to determine hydraulic permeability in Darcy's linear equation. Then, also unsaturated samples under steady state condition have been investigated, e.g.. in [3], [2]. Dynamic unsaturated flow with equilibria measurements have been investigated, e.g., in [4], [2]. In [6] and [11] transient measurements from sample inside have been used. We have investigated the determination of soil parameters under centrifugation using only noninvasive measurements in [8], [10], [14], [13] and [15].

In [11] (see also citations there) the equilibrium analysis for a set of rotational speeds has been used to determine soil parameters. The distribution of saturation in equilibria (linked with the corresponding rotational speeds) was measured via electrical signals from electrodes installed in the sample. Transient measurements have been also applied there. At the beginning the sample was fully saturated and the outflow from the sample was controlled. The column experiments in determination of soil parameters have been applied in [7].

Determination of soil parameters under the pressure/saturation informations from sample inside is more reliable, but technically difficult, especially in transient measurements. The presence of only inflow/outflow informations leads to very ill-posed problem and this must be compensated by very accurate numerical solution of direct problem and suitable experiment scenario.

In our papers [10], [14], [15] we discussed another 1D centrifugation scenario, where non-invasive measurements of flow characteristics have been used and their sufficiency in determining procedure have been demonstrated. The used numerical method was original and based on the interface modeling. This we do not know in more then one dimensional case.

In the present contribution we focus on both: gravitation driving force and the centrifugal driving force. Unlike in previous papers, we consider more realistic 3D rotationally symmetric sample.

In Section II we introduce the mathematical model and in Section III we present our numerical method. Solution of inverse problem will be presented in Section IV. In Section V we discuss numerical experiments. Finally, conclusions are presented in Section VI.

II. Mathematical model

Our sample is a cylinder with radius R ([cm]) and height Z ([cm]). We transform the mathematical model using cylindrical coordinates (r, z). Then the governing PDE for infiltration reads as follows

$$\partial_t \theta(h) = \frac{1}{r}\partial_r(rK(h)\partial_r h) + \partial_z(K(h)(\partial_z h - \beta)) \quad (1)$$

where the saturation θ, depending on pressure head h ([cm]), is of the form

$$\theta(h) = \theta_r + (\theta_s - \theta_r)\theta_{ef}(h), \quad (2)$$

with irreducible saturation θ_r, porosity θ_s and effective saturation $\theta_{ef}(h)$. We consider the fundamental saturation-pressure law in terms of van Genuchten-Mualem empirical ansatz ($h \leq 0$ in unsaturated zone, in saturated zone $\theta_{ef} = 1$, $h > 0$)

$$\theta_{ef}(h) = \frac{1}{(1 + (\alpha h)^n)^{\frac{1}{m}}}, \quad (3)$$

where α ($[cm^{-1}]$) and $n,\ m = 1 - \frac{1}{n}$ are soil parameters. The hydraulic permeability $K = K(h)$ ($[cm/s]$) is in van Genuchten-Mualem ansatz

$$K(h) = K_s\left(\theta_{ef}(h)\right)^{\frac{1}{2}} . \left(1 - \left(1 - \left(\theta_{ef}(h)\right)^{m}\right)^{\frac{1}{m}}\right)^2, \quad (4)$$

where K_s ($[cm/s]$) is a hydraulic permeability for saturated porous media (also soil parameter), i.e., $K_s = K(0)$. In the gravitational mode $\beta = 1$ and in the centrifugation mode (coordinate $-z$ is in the direction of centrifuge arm) we have

$$\beta = \frac{\omega^2}{g}\left(L - z\right)$$

where L ([cm]) is the distance of sample bottom from the centrifugation axis, ω ($[s^{-1}]$) is the rotational speed and g ($[cm/s^2]$) is the gravitational acceleration. Denote by D ($[cm]$) the distacnce between the sample and the collection chamber bottoms.

The flux $\mathbf{q}$ ($[cm/s]$) in cylindrical coordinates is of the form

$$\mathbf{q} = -(q_r, q_z)^T, \quad (5)$$

$$q_r = K(h)\partial_r h,\ q_z = K(h)(\partial_z h - \beta).$$

We note that our model includes both saturated (elliptic PDE) and unsaturated (parabolic PDE) zones. We consider initially (at $t = 0$) the dry sample $h = -\infty$), but in the numerical experiments we use $h = -300$. The top of our sample $\Gamma_{top} = \{r \in (0, R), z = Z\}$ is isolated, i.e., we consider $q_z = 0$ and the same condition we consider on the part $\{r \in (R1, R), z = 0\}$ of the bottom. Through the part $\Gamma_{out} = \{r \in (0, R1), z = 0\}$ the infiltrated water can outflow to the collection chamber, i.e. we consider $h\partial_z h = 0$ on Γ_{out}. This condition has to be interpreted in the following way. In the points from Γ_{out} where $h < 0$ the boundary conditiuon is $\partial_z h = 0$ (see q_z in (5)), otherwise $h = 0$.

The boundary condition on the sample mantel $\Gamma_{mant} = \{r = R, z \in (0, Z)\}$ reflects the hydrostatic pressure generated by the water level $H(t) \geq 0$ (H ([cm]) measured from the top of the sample) at the coordinate $0 \leq z \leq Z$. Then our boundary condition on Γ_{mant} in gravitation mode is

$$h(t, R, z) = H(t) + (Z - z) \quad (6)$$

Due to the mass ballance argument, the change in $H(t)$ reflects the infiltration flux through Γ_{mant} for $t > 0$. Thus, our system is closed by ODE

$$\dot{H}(t) = -Q\int_{\Gamma_{mant}} q_r\, d\Gamma_{mant} \quad (7)$$

where Q is the ratio of the areas of Γ_{top} and the crossection of inflow chamber. The amount of outflow water M_{out} ($[cm^3/s]$) in the collection chamber is given by

$$M_{out}(t) = \int_0^t \int_{\Gamma_{out}} q_z\, d\Gamma_{out} dt$$

which could be expressed in terms of water level

$$H_{out}(t) = Q_1 M_{out}(t),$$

where Q_1 is the ratio of areas Γ_{out} of the crossection area and collection area of the collection chamber.

In the case of centrifugation, the condition (6) is replaced by

$$h(t, R, z) = \int_z^{H(t)+Z} \frac{\omega^2}{g}(L - p)dp.$$

We note that in centrifugation mode the gravitational force is neglected.

III. Numerical method

Our accurate and efficient numerical method in 1D substantially used mathematical model (in terms of ODE) describing the interfaces between fully saturated, partially saturated and dry zones of the sample. In the more dimensional case we do not have such model. Therefore, more discretization grid points have to be used. We apply devised linearization and regularization to manage serious difficulties concerning degeneracy and strong nonlinearities appearing in a small neighbourhood of mentioned interfaces. The solution has very sharp, moving front between partially saturated and dry zones.

We have developed two different approximation schemes. In the first one we apply space discretizatioin based on a finite volume method and flexible time stepping in time variable. The obtained nonlinear system of algebraic equations is linearized by quasinewton method. We follow the idea in M. A. Celia and Z. Bouloutas in [12], which was also applied in the well known software HYDRUS [9]. In the second method, after space discretization (based on finite volume method) we reduce our system to the ODE system. In fact, the obtained ODE system is singular and some regularization was applied. On the other hand all nonlinearities are approximated accurately. Both methods give nearly the same results, but the first one is much quicker and therefore is more suitable for solving inverse problems.

A. Approximation of governing equations

Consider the grid points $(r_i, z_l) = (i\Delta r,\ l\Delta z)$ for $i \in \left\{0, 1, \dots, \frac{R}{\Delta r}\right\}$ and $l \in \left\{0, 1, \dots, \frac{Z}{\Delta z}\right\}$ with the fixed space step $(\Delta r, \Delta z)$ and flexible time step Δt_j which will be modified in the iteration procedure. To construct approximation scheme linked with the grid point (r_i, z_l, t_{j+1}), we integrate (1) over the volume

$$V_{i,l,j} = (r_i - \frac{\Delta r}{2},\ r_i + \frac{\Delta r}{2})\times$$

$$(z_l - \frac{\Delta z}{2},\ z_l + \frac{\Delta z}{2}) \times (t_j,\ t_j + \Delta t_j).$$

We apply integration by parts in corresponding terms and approximate

$$\partial_x h(r_{i+1/2}, z_l, t_j) \approx \frac{h(r_i + 1, z_l, t_j) - h(r_i, z_l, t_j)}{\Delta r}$$

and

$$h(r_{i+1/2}, z_l, t_j) \approx \frac{h(r_i+1, z_l, t_j) + h(r_i, z_l, t_j)}{2}.$$

Similarly we approximate $\partial_r h(r_{i-1/2}, z_l, t_j),\ h(r_{i-1/2}, z_l, t_j)$. In the same way we approximate $\partial_z h$ and the values of $K(h)$ in the middle grid points, where the average of values h in neighbouring grid points is used. Then our approximation scheme reads as follows

$$\frac{(\theta_{i,l}^{j+1} - \theta_{i,l}^{j})}{\Delta t_j} = \frac{r_{i+\frac{1}{2}}}{r_i} K_{i+\frac{1}{2},l}^{j+1} \frac{h_{i+1,l}^{j+1} - h_{i,l}^{j+1}}{(\Delta r)^2} - \tag{8}$$

$$\frac{r_{i-\frac{1}{2}}}{r_i} K_{i-\frac{1}{2},l}^{j+1} \frac{h_{i,l}^{j+1} - h_{i-1,l}^{j+1}}{(\Delta r)^2} +$$

$$\frac{1}{\Delta z} K_{i,l+\frac{1}{2}}^{j+1} \left(\frac{h_{i,l+1}^{j+1} - h_{i,l}^{j+1}}{\Delta z} - \beta_l \right) -$$

$$\frac{1}{\Delta z} K_{i,l-\frac{1}{2}}^{j+1} \left(\frac{h_{i,l}^{j+1} - h_{i,l-1}^{j+1}}{\Delta z} - \beta_l \right),$$

where $\beta_{i,l} = 1$ in the case of gravitation mode and in the centrifugation mode we have

$$\beta_{i,l} = \frac{\omega^2}{g} (L - z_l).$$

This is strongly nonlinear system because of (3). We linearize it by means of quasinewton iterations with iteration parameter k (see [12]). The left hand part in (8) we linearize by

$$\frac{\theta_{i,l}^{j+1,k+1} - \theta_{i,l}^{j}}{\Delta t_j} = \tag{9}$$

$$C_{i,l}^{j+1,k} \frac{h_{i,l}^{j+1,k+1} - h_{i,l}^{j+1,k}}{\Delta t_j} + \frac{\theta_{i,l}^{j+1,k} - \theta_{i,l}^{j}}{\Delta t_j} \equiv$$

$$L_{i,l}^{j+1,k}$$

where

$$C_{i,l}^{j+1,k} = \left(\frac{\mathrm{d}\theta}{\mathrm{d}h} \right)_{i,l}^{j+1,k}.$$

On the right hand side in (8) we consider the values $h^{j+1,k}$ (from previous iteration step) in $K(h)$. Our linearization reads as follows

$$L_{i,l}^{j+1,k} =$$

$$\frac{r_{i+\frac{1}{2}}}{r_i} K_{i+\frac{1}{2},l}^{j+1,k} \frac{h_{i+1,l}^{j+1,k+1} - h_{i,l}^{j+1,k+1}}{(\Delta r)^2} - \tag{10}$$

$$\frac{r_{i-\frac{1}{2}}}{r_i} K_{i-\frac{1}{2},l}^{j+1,k} \frac{h_{i,l}^{j+1,k+1} - h_{i-1,l}^{j+1,k+1}}{(\Delta r)^2} +$$

$$\frac{1}{\Delta z} K_{i,l+\frac{1}{2}}^{j+1,k} \left(\frac{h_{i,l+1}^{j+1,k+1} - h_{i,l}^{j+1,k+1}}{\Delta z} - \beta_l \right) -$$

$$\frac{1}{\Delta z} K_{i,l-\frac{1}{2}}^{j+1,k} \left(\frac{h_{i,l}^{j+1,k+1} - h_{i,l-1}^{j+1,k+1}}{\Delta z} - \beta_l \right).$$

Thus (9),(10) represent a linear algebraic system in terms of $h_{i,l}^{j+1,k+1}$. The iteration will stop for $k = k^*$ when

$$||\mathbf{h}^{j+1,k+1} - \mathbf{h}^{j+1,k}|| < tollerance.$$

Then we put $\theta_{i,l}^{j+1} = \theta_{i,l}^{j+1,k^*}$ corresponding to $h_{i,l}^{j+1,k^*}$ (see (3)). The same approximation strategy we use at boundary points where the control volume $V_{i,l,j}$ is reduced.

B. Numerical acceleration

The computational process can be significantly accelerated by a suitable choice of time step and starting value $\mathbf{h}^{(k=0)}$. Starting point can be constructed via interpolation of few (cca 5) values from previous time steps of $\mathbf{h}$.

Additional speed increase can be reached by damping technique and appropriate choice of time step depending on the number of iterations in previous iteration procedure. We have to note (and it is very surprising) that by suitable choice of previous atributes in iteration procedure it is possible to reach significant reduction in the computational time. Without damping the iteration process can even fail.

The tunning of damping parameters should be appropriately updated with the change of the driving force.

C. Approximation by ODE system

We construct the governing ODE linked with the grid point (r_i, z_l) (similarly as before) integrating (1) over control volume

$$V_{i,l} = (r_i - \frac{\Delta r}{2},\ r_i + \frac{\Delta r}{2}) \times$$

$$(z_l - \frac{\Delta z}{2},\ z_l + \frac{\Delta z}{2}).$$

The left hand side of (1) we approximate (in (r_i, z_l)) by

$$\frac{\partial \theta_{i,l}(t)}{\partial h_{i,l}(t)} \partial_t h_{i,l}(t) \Delta r \Delta z. \tag{11}$$

The right hand side in (1) we approximate using integration by parts similarly as before. Then we obtain

$$\frac{r_{i+\frac{1}{2}}}{r_i} K_{i+\frac{1}{2},l}^{j+1,k} \frac{h_{i+1,l}(t) - h_{i,l}(t)}{(\Delta r)^2} - \tag{12}$$

$$\frac{r_{i-\frac{1}{2}}}{r_i} K_{i-\frac{1}{2},l}^{j+1,k} \frac{h_{i,l}(t) - h_{i-1,l}(t)}{(\Delta r)^2} +$$

$$\frac{1}{\Delta z} K_{i,l+\frac{1}{2}}^{j+1,k} \left(\frac{h_{i,l+1}(t) - h_{i,l}(t)}{\Delta z} - \beta_l \right) -$$

$$\frac{1}{\Delta z} K_{i,l-\frac{1}{2}}^{j+1,k} \left(\frac{h_{i,l}(t) - h_{i,l-1}(t)}{\Delta z} - \beta_l \right).$$

Thus, (11) and (12) represents a nonlinear ODE system of the form

$$M(t, \mathbf{h}) \frac{d\mathbf{h}}{dt} = \mathbf{F}(t, \mathbf{h})$$

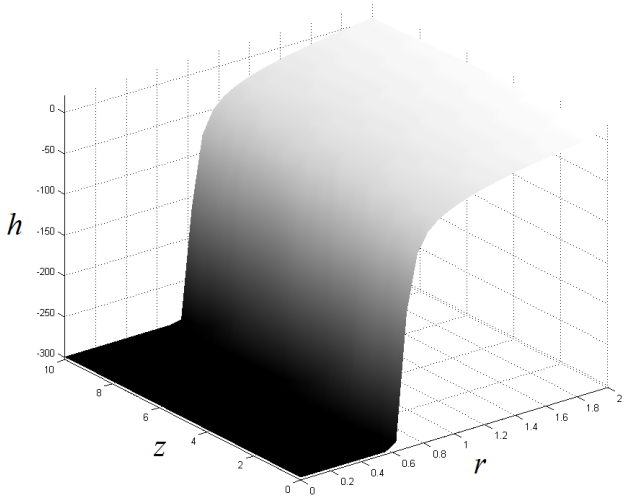

Fig. 2 Pressure at $T = 20s$, gravitation

which can be solved by (professional) solver for stiff ODE. In fact, matrix M should be regularized, because it degenerates (in saturated zone where $\theta(t) = \theta_s$). In numerical realization we replace the zero values on diagonal by a small value $\epsilon = 10^{-5}$. The numerical solutions with

$$\epsilon = 10^{-6},\ \epsilon = 10^{-7}$$

differ from previous one only on 5 -th decimal place. Because of the degeneracy the computing time significantly increases with decrease of ϵ. Moreover, the ODE system is too large considering relatively small space discretization.

The numerical solutions obtained by both numerical methods coincide on 5 decimal digits. However, the first method is much more quicker even when smaller space step is used. Therefore, the first method is more suitable for solving inverse problems, where many iterations with direct solutions are expected.

D. Numerical experiments

The *standard* model data used in numerical experiments are:

$$Z = 10,\ R = 2,\ H(0) = 5,\ R_1 = 1,$$

$$\alpha = -0.0189,\ n = 2.81,\ m = 1 - \frac{1}{n},$$

$$K_s = 2.4 \times 10^{-4},\ \theta_r = 0.02,\ \theta_s = 0.38,\ \omega = 20,$$

$$L = 40,\ D = 5,\ Q_{top} = \pi R^2,\ Q = \frac{1}{4}.$$

In numerical solutions we use the space discretization using $\Delta z = \frac{Z}{30}\ \Delta r = \frac{R}{30}$ which seems to be satisfactory for accurate solution for our purposes for inverse problems. The same discretization we have used in following figures.

In case of the gravitational force, Fig. 2 express pressure h graphically at a time moment $T = 20s$. More detailed information about the solution can be seen in Fig. 3, where the contour lines are drawn. This figure represents the solution at time

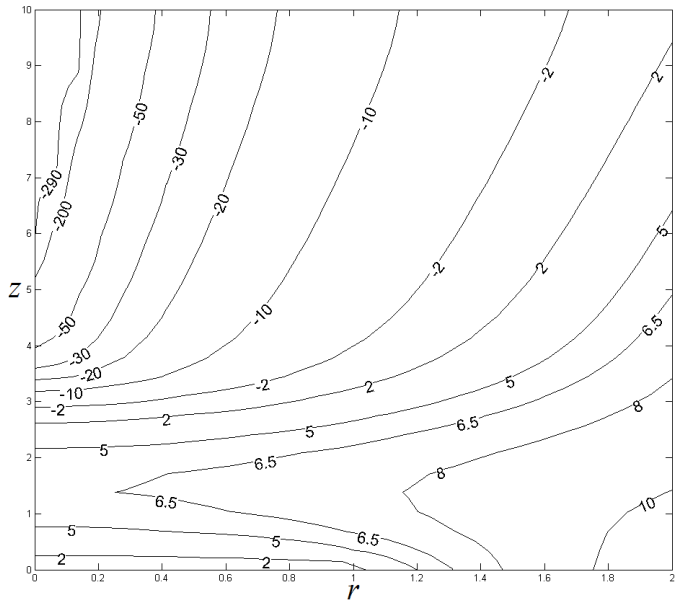

Fig. 3 Pressure contour lines at $T = 40s$, gravitation

$T = 40s$, where the influence of the water outflow can be noticed and regions of dry, partially saturated and fully saturated zones can be recognized.

The water level $H(t)$ and outflow $50000 M_{out}(t)$ are drawn in Fig. 3 (full lines).

In case of centrifugation, Fig. 5 express pressure graphically at a time moment $T = 20s$. The corresponding contour lines are plotted in the Fig. 6. Contour lines are very useful for the comparison of gravitational (at $T = 40s$) and centrifugal (at $T = 20s$) infiltration scenarios.

The time evolution of the water level $H(t)$ ($t \in (0, 20)$) and the time evolution of the amount of outflow water $M_{out}(t)$ ($t \in (0, 11)$) is ploted in Fig. 7. The time evolution of centrifugal force is drawn in Fig. 8.

Very similar picture as in Fig. 2 and 5 can be obtained by plotting effective saturation θ instead of the pressure h (see (3)). We can see the sharp front of infiltrated water. This moving front causes numerical difficulties. We can observe the acceleration of the infiltration procedure, especially at the outflow. Pressure contour lines in Fig. 3 are obtained at $T = 40s$, while water level $H(t)$ and outflow M_{out} (with same model data) are obtained at $T = 25s$. The corresponding water flow front reaches the otflow position at the sample bottom after $15s$. Consequently, the amount of outflow M_{out} is very small. The outflow at centrifugation mode (see Fig. 7) is significantly larger, because the water flow front reaches the outflow position at $T = 5s$ and the centrifugal driving force is there 20 times bigger as the gravitation force.

IV. Solution of the inverse problem

In the solution of the inverse problem we minimize the discrepancy between the measured and computed data. Minimiza-

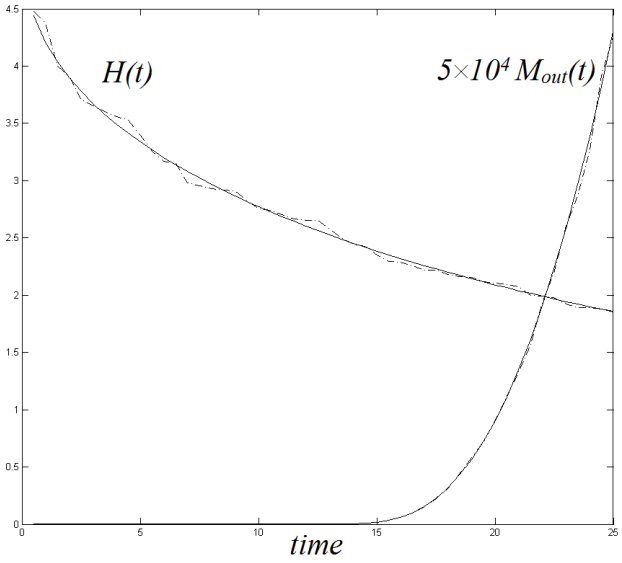

Fig. 4 Inflow-outflow, gravitation

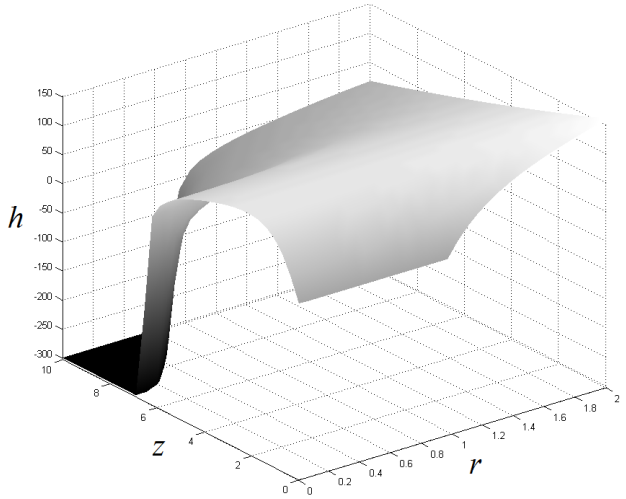

Fig. 5 Pressure at $T = 20s$, centrifugation

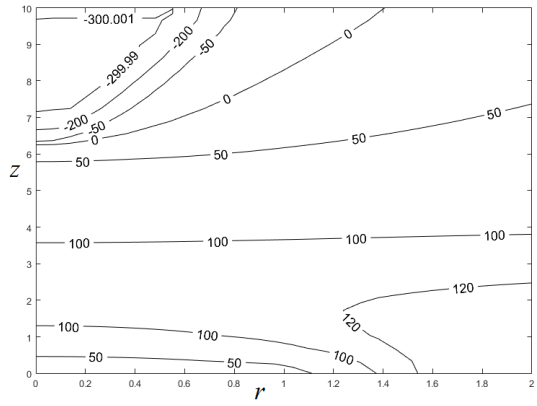

Fig. 6 Pressure contour lines at $T = 20s$, centrifugation

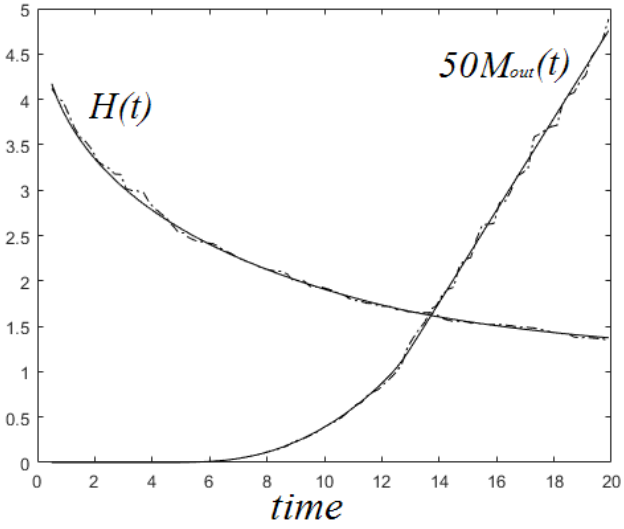

Fig. 7 Input-output water, centrifugation

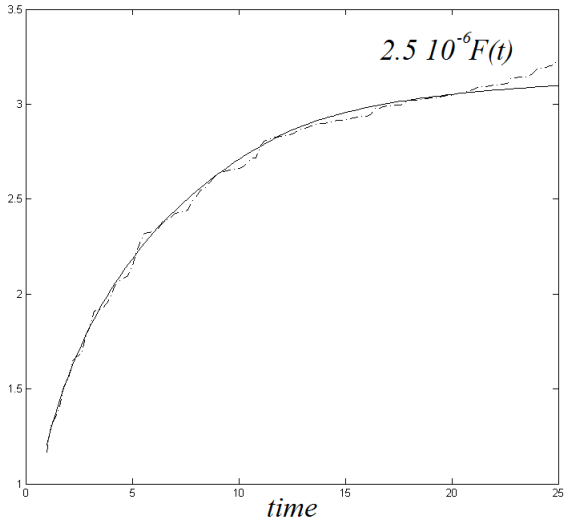

Fig. 8 Centrifugal force $F(t)$

Table 1 Optimal parameters with 3 different noises

α	n	$K_s \times 10^4$
-0.015359	2.7636	2.168
-0.018427	2.7077	
-0.018163	2.9865	2.310
-0.019119	2.8467	
-0.019417	2.7421	2.446
-0.018907	2.8037	

tion problem is solved in an iterative way using well known solver *fminsearch* from the MATLAB toolbox. At solving inverse problems determining soil parameters ($\alpha,\ n,\ K_s$) we consider starting points different from standard data.

In the experiment below we demonstrate applicability of our method in determining soil parameters. Firstly, we prepare standard data $H(t)$, $M_{out}(t)$ and $F(t)$ in 50 uniformly distributed time sections in the observation interval $[0.5, 25]$. Then using random function we add 5% noise to our data. Then the noised data are sorted, because the nature of the experiment dictates that data are monotonous. This will represent measuring data.

Secondly, we *forget* standard soil parameters and use different starting points for them. As a result of the inverse procedure (by minimization of discrepancy between measured and computed data) we obtain "optimal" solution. Our starting points consist of all combinations of parameters

$$\alpha \in \{-0.017,\ -0.02\},$$

$$n \in \{2.6,\ 3\},$$

$$K_s \in \{2 \times 10^{-4},\ 2.8 \times 10^{-4}\}.$$

A. Experiments with gravitational force

Fig. 4 shows standard data (full line) and noised data (dott dash line) obtained in gravitation mode. The optimal parameters of inverse problems using this measured data are in the first pair of rows in table 1.

The parameter K_s can be determined distinctively by simple experiment with fully saturated sample. Therefore we also solved inverse problems for only 2 parameters α, n assuming $K_s = 2.4 \times 10^{-4}$.

In both cases the optimal solution does not depend on the choice of a starting point (the relative differences are less then 10^{-5}). However, the small dependance on noise generation is observed. The table 1 shows optimal parameters for different noises. The pairs of succesive rows correspond to the standard data with the same noise. In each pair, the second row represents a solution of inverse problem with only 2 parameters.

B. Experiments with centrifugal force

Aditionally to the measurements of $H(t)$ and $M_{out}(t)$ we can measure the centrifugal force $\frac{\omega^2}{g}F(t)$ linked with the movement of water along the centrifuge arm. Here,

Table 2 Optimal parameters in gravitation mode

α	n	$K_s \times 10^4$
-0.02	3.	2.
-0.01841	2.834	2.402
-0.02	3.	2.8
-0.02256	2.857	2.511
-0.02	2.6	2.
-0.01886	2.789	2.418
-0.02	2.6	2.8
-0.02051	2.795	2.455
-0.017	3.	2.
-0.01823	2.823	2.404
-0.017	3.	2.8
-0.02231	2.772	2.444
-0.017	2.6	2.
-0.01880	2.799	2.398
-0.017	2.6	2.8
-0.01867	2.761	2.412

$$F(t) = F_{inj}(t) + F_s(t) + F_{out},$$

where

$$F_{inj}(t) = \frac{Q_{top}}{2}\left((H(t)+L)^2 - H(t)^2)\right) +$$

$$\frac{Q_{top}Q}{2}\left(L^2 - (L-Z)^2\right)$$

is linked with water in the injection chamber. Contribution of water in the sample is

$$F_s(t) =$$

$$\frac{1}{2}(\theta_s - \theta_r)\left(\int_0^R \int_0^Z 2\pi r(L-z)\theta(r,z,t)drdz\right)$$

and

$$F_{out}(t) = \frac{1}{2}\left((L+D)^2 - (L+D-M_{out}(t))^2\right).$$

In Fig. 7 and Fig. 8 we plot the standard data (full line) and noised data (dott dash line) obtained in centrifugation mode. In Fig. 8 we plot only scaled value of F and call it as centrifugal force.

We use the same starting parameters as in gravitation mode and apply the same optimization procedure. The obtained *optimal* values are presented in Table 2. There the pairs of starting and optimal parameters are included for each starting point.

V. Analysis of obtained results in experiments

Numerical experiments demonstrate efficiency of our numerical method also in more dimensional case using only noninvasive measurements. The 5% noise in our measurements effects the $5-6\%$ defect in case with two soil parameters $\alpha,\ n$. In the case with 3 soil parameters the defect reaches up to 15%.

We have remarked very low dependance of optimal solution on starting points in the gravitation mode. Greater dependance is linked to the type of generated noise. In case of centrifugation we have observed more local minima points, especially with starting points containing $n=3,\ K_s=2.8\,10^{-4}$. In that case the defect was up to 13%. In other starting points the defect reaches up to 10%, so the measurement of centrifugal force stabilize the determination procedure. The dependance on starting points is higher than in gravitation mode and thus Table 2 contains pairs of starting points and optimal ones.

In practical applications we can combine both measurements from gravitation and centrifugation mode in the same determination procedure. Moreover, we can change the rotaional speed during the experiment. The reason is, that the saturation distribution in the sample and amount of water in the collection chamber can be changed more dynamically, which could improve parameter determination. This have been implemented in our previous centrifuge version in 1D (see [10]).

VI. Conclusions

An accurate and efficient numerical method was developed for solving the direct infiltration problem in unsaturated/saturated porous media in 3D. This method is a good candidate for solving the inverse problem in order to determine soil parameters in capillary-pressure flow model. The suggested experiment scenario completed by our numerical method seems to be suitable instrument in determination of soil parameters requiring only noninvasive global inflow/outflow characteristics (eventually, centrifugal force). Effectiveness (computing time) of our numerical method is strongly dependent on inner tunning parameters which need updating with stronger change of model data, e.g., when changing from gravitation to centrifugation mode. When the transient measurements of centrifugal force are affected by more than 5% of error, then this information in determination procedure is contraproductive and we drop out its measurements.

More local minima appear in centrifugation mode and thus various starting parameters have to be used and evaluated.

In the next research we aim to increase the reliability of determined soil parameters by combining the measurements of gravitation and centrifugation experiments using the same sample and under the same model data.

Our method can be also used in sacenario, when we start with fully saturated sample and empty injection chamber. We can also isolate the bottom of the sample and let it reach equilibrium. Especially, in case of centrifugation we can create series of equilibria and from their information obtain soil parameters as in 1D (see [13]).

References

[1] J. Bear and A. H.-D. Cheng, *Modeling Groundwater flow and Contaminant Transport.* Dordrecht-Heidelberg-London-New York, Springer, ISBN 978-1-4020-6681-8, 2010.

[2] R. J. Nimmo, and K. A. Mello," Centrifugal techniques for measuring saturated hydraulic conductivity,"*Water Resour. Res.*, 27(6), 1363-1261, 1991.

[3] J. R. Nimmo, J. Rubin, and D. P. Hammermeister," Unsaturated flow in a centrifugal field: Measurement of hydraulic conductivity and testing of Darcy's law," *Water Resour. Res.*, 23(1), 124-137, 1987.

[4] P. J. Culligan, D. A. Barry, and J.Y. Parlange," Scaling unstable infiltration in the vadose zone," *Can. Geotech. J.*, 34(3), 466-470, 1997.

[5] H. Nakajima, E. D. Mattson, and A. T. Stadler," Unsaturated hydraulic properties determined from geocentrifuge tests," *Eos Trans. AGU*, 84(46), Fall Meet. Suppl., Abstract H22A-0908, 2003.

[6] C. Savvidou, and P. J. Culligan," The application of centrifuge modeling to geo-environmental problems," *Proc. Inst. Civ. Eng. Geotech. Eng.*, 131, 152-162, 1998.

[7] S. Bitterlich, W. Durner, SC. Iden and P. Knabner," Inverse estimation of the unsaturated soil hydraulic properties from column outflow experiments using free-form parametrizations,"*Vadose Zone Journal* 3, pp. 971-981, 2004.

[8] GK D. Constales, and J. Kačur," Determination of soil parameters via the solution of inverse problems in infiltration," *Computational Geosciences* 5 , pp. 25-46, 2004.

[9] J. Šimunek, M. Šejna, H. Saito, M. Sakai, and M. Th. van Genuchten," Heat, and Multiple Solutes in Variably Saturated Media." *The Hydrus-1D Software Package for Simulating the Movement of Water,* 2013.

[10] J. Kačur, B. Malengier, and P. Kišon," A numerical model of transient unsaturated flow under centrifugation based on mass balance," *Transport in Porous Media,* Vol.87,3, pp. 793-813, 2011.

[11] J. Šimunek, and J. R. Nimo," Estimating soil hydraulic parameters from transient flow experiments in a centrifuge using parameter optimization technique," *Water Resour. Res.* 41, W04015, 2005.

[12] M. A. Celia, and Z. Bouloutas," A general mass-conservative numerical solution for the unsaturated flow equation," *Water Resour. Res.* 26, pp. 1483-1496, 1990.

[13] J. Kačur, B. Malengier, and P. Kišon," Using global characteristics of a centrifuge outflow experiment to determine unsaturated soil parameters," *Mathematical Problems in Engineering,* ID 163020,23 pages, 2011.

[14] J. Kačur, B. Malengier, and P. Kišon," Unsaturated-saturated flow in porous media under centrifugation," *Numerical analysis of Heat and Mass Transfer in Porous Media,* Berlin,Springer, pp. 275-295, 2012.

[15] J. Kačur, J. Minar, and H. Budačova, ”Determination of soil parameters based on mathematical modelling of centrifugation,” *In International Journal of Mathematical Modelling and Numerical Optimisation,* vol. 5, no.3, pp.153-170,2014.